Energy Materials

Supplementary Material

Interlayer expansion and conductive networking of MoS_2 nanoroses mediated by bio-derived carbon for enhanced potassium-ion storage

Shuo Zhang[1,#], Zonggui Yin[1,#], Lili Wang[1,*], Mengyao Shu[1], Xin Liang[1], Sheng Liang[1], Lei Hu[1], Chonghai Deng[1], Kunhong Hu[1], Xiaobo Zhu[2,*]

[1]Key Laboratory of Materials and Technologies for Advanced Batteries, LIB Technology Center of Anhui Province, Hefei University, Hefei 230601, Anhui, China.
[2]College of Materials Science and Engineering, Changsha University of Science and Technology, Changsha 410114, Hunan, China.
[#]Authors contributed equally.

Correspondence to: Dr. Lili Wang, Key Laboratory of Materials and Technologies for Advanced Batteries, LIB Technology Center of Anhui Province, Hefei University, Hefei 230601, Anhui, China. E-mail: wangll@hfuu.edu.cn; Dr. Xiaobo Zhu, College of Materials Science and Engineering, Changsha University of Science and Technology, Changsha 410114, Hunan, China. E-mail: xbzhu@outlook.com

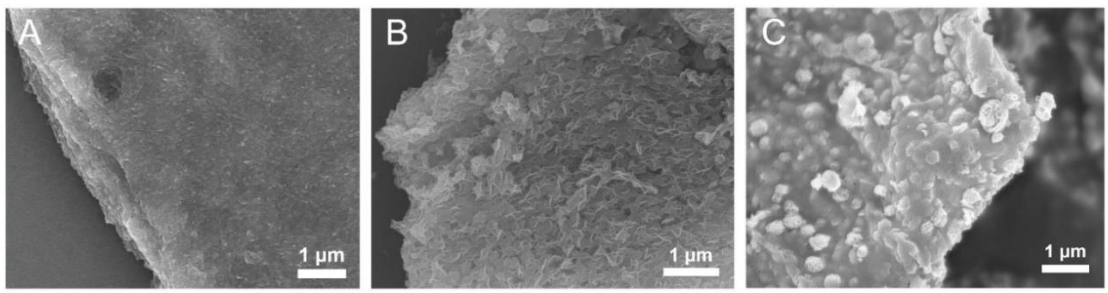

Supplementary Figure S1. (A) SEM images of MoS_2/AB composites collected after hydrothermal reaction of (A) 6 h, (B) 12 h, and (C) 18 h

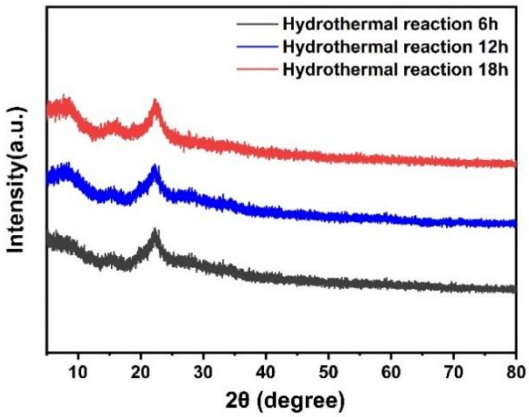

Supplementary Figure S2. XRD patterns of MoS_2/AB composites collected after hydrothermal reaction of (A) 6 h, (B) 12 h, and (C) 18 h

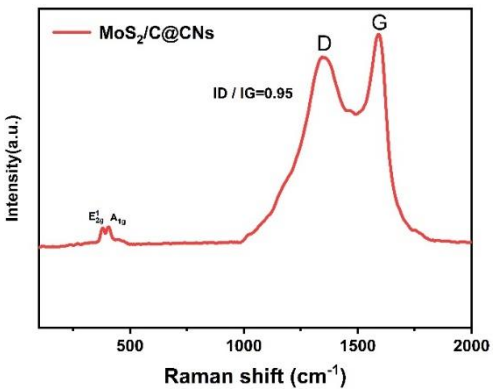

Supplementary Figure S3. Raman spectrum of MoS_2/C@CNs

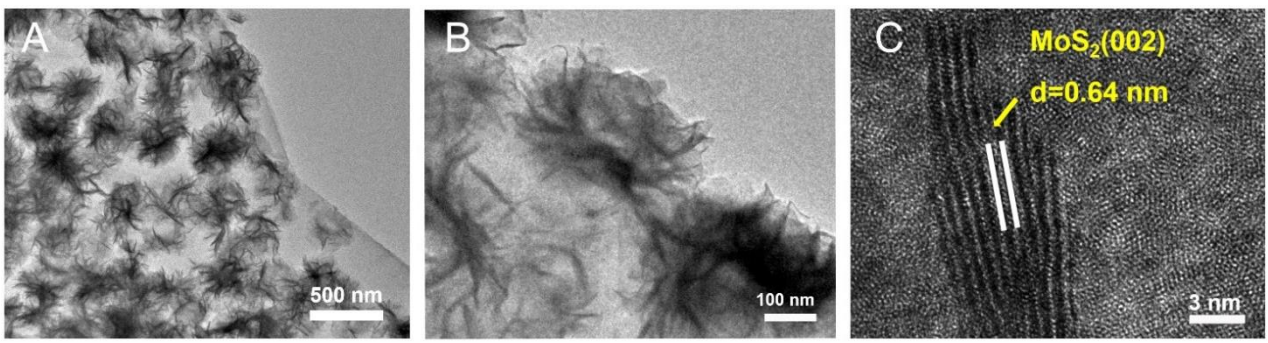

Supplementary Figure S4. (A, B) TEM and (C) HR-TEM images of MoS_2/C

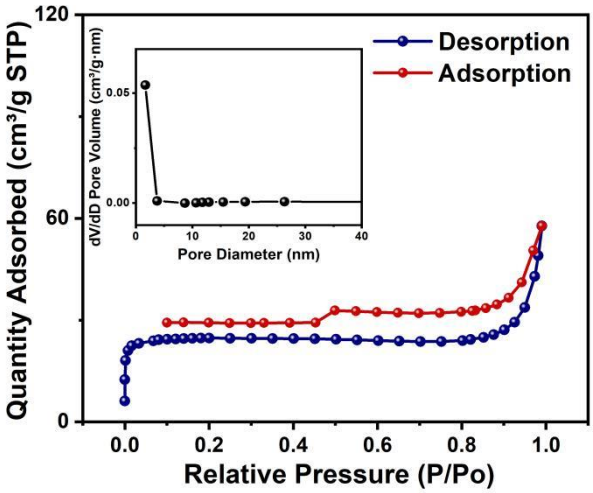

Supplementary Figure S5. N_2 adsorption-desorption isotherms of MoS_2/C

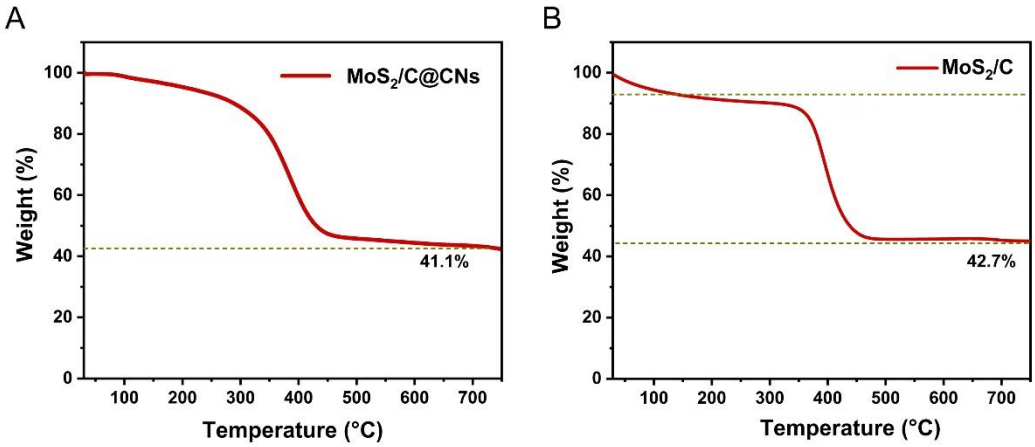

Supplementary Figure S6. TGA analysis of (A) MoS_2/C@CNs and (B) MoS_2/C from 30 to 750 °C in air

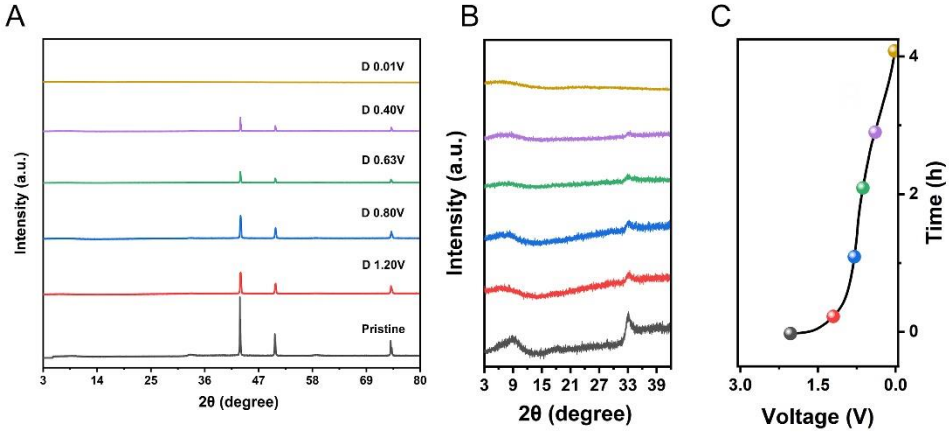

Supplementary Figure S7. *Ex-situ* XRD analysis on MoS_2/C@CNs electrode during discharging: (A) XRD patterns at angles of 3-80°, (B) Zoomed XRD patterns at angles of 3-39°, (C) corresponding voltage-time curves

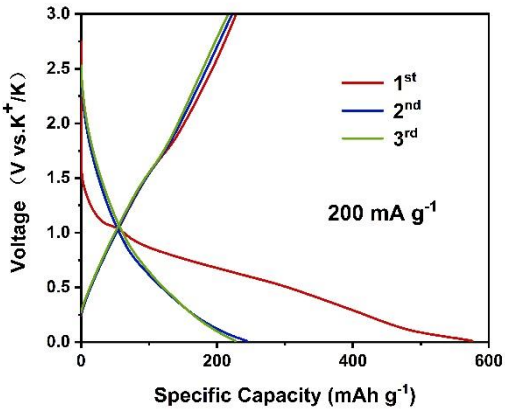

Supplementary Figure S8. Discharge-charge profiles of MoS_2/C tested at 200 mA g^{-1}

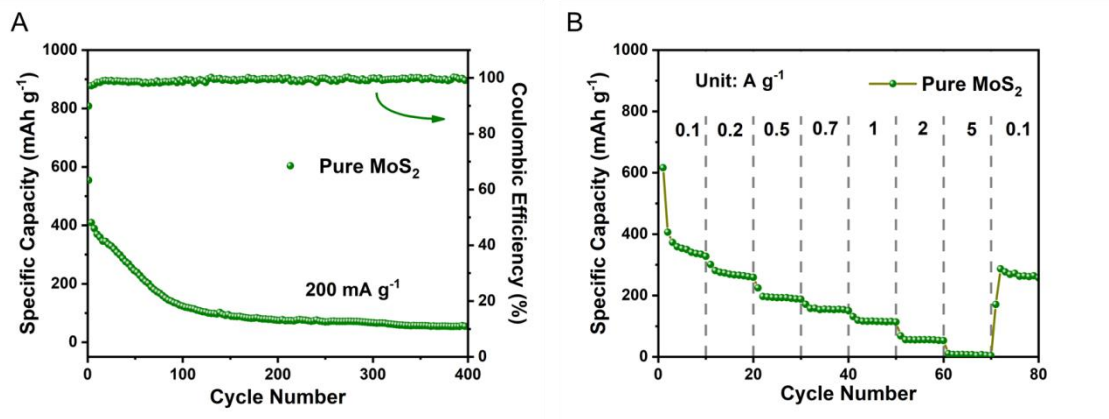

Supplementary Figure S9. Electrochemical performance of pure MoS_2 electrode. (A) cycle performance at 200 mA g^{-1} and (B) Rate performance

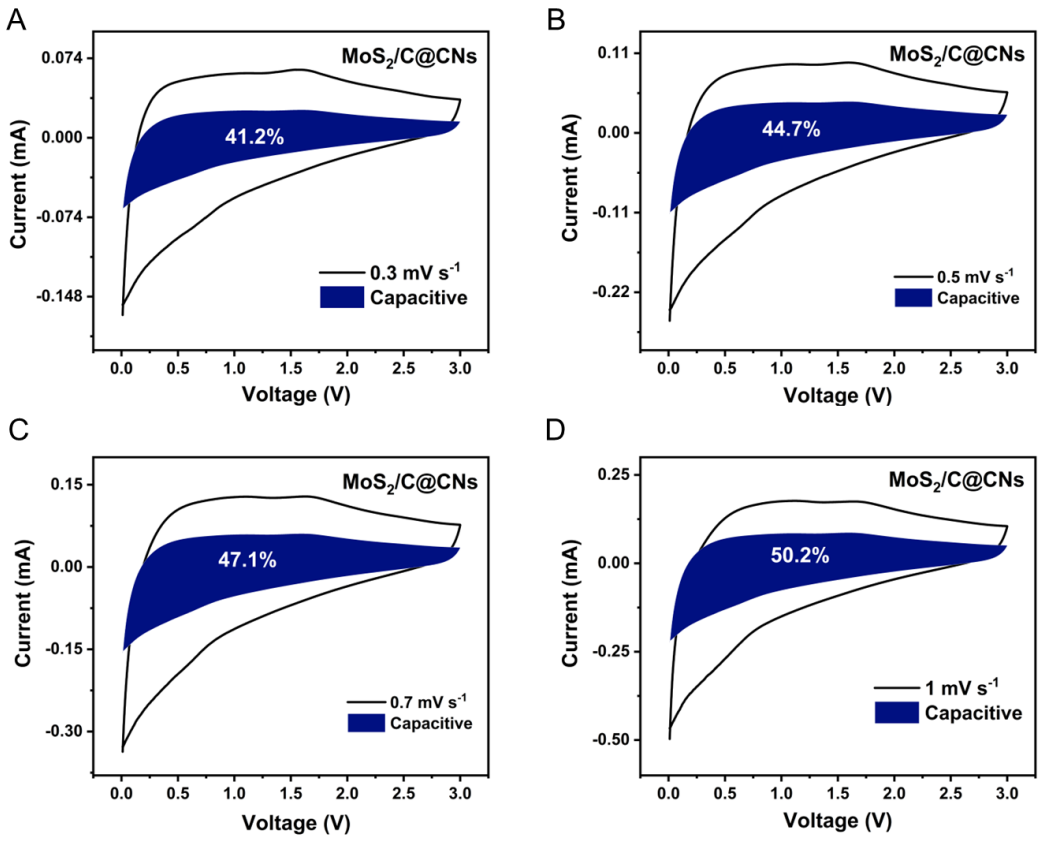

Supplementary Figure S10. (A-D) Capacitive contributions at various scan rates of 0.3, 0.5, 0.7, 1.0 mV s^{-1} for MoS_2/C@CNs.

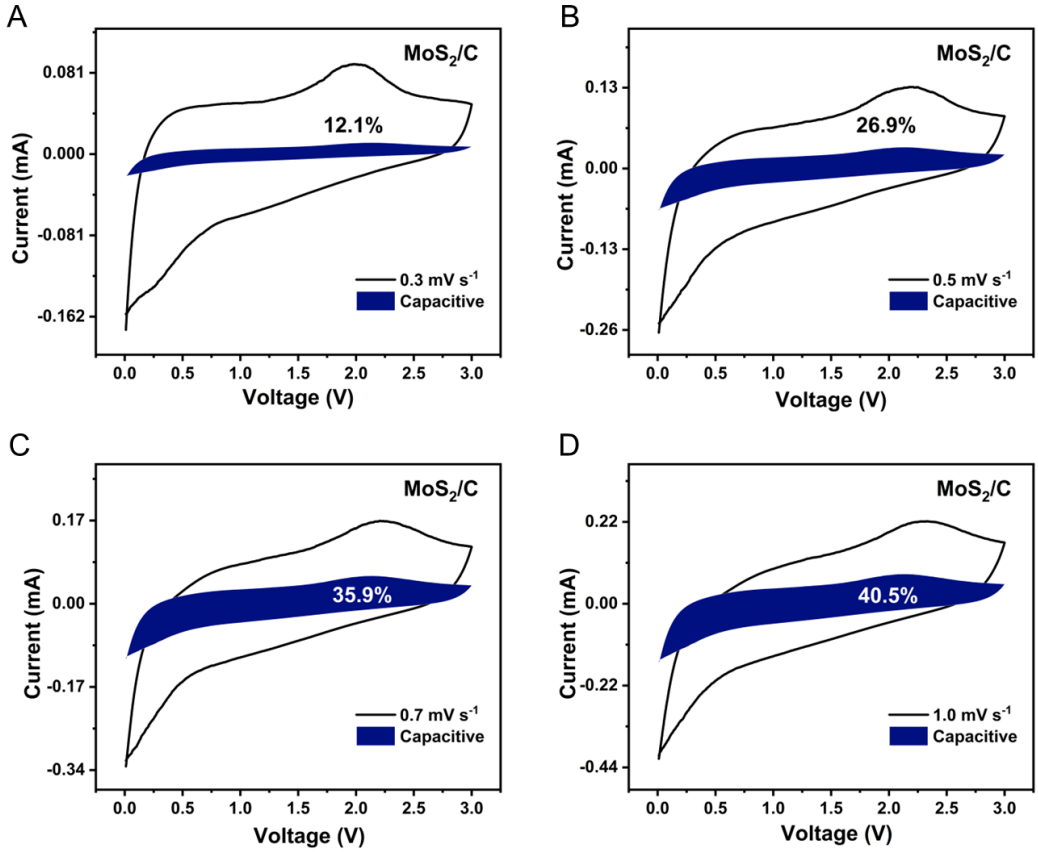

Supplementary Figure S11. (A-D) Capacitive contributions at various scan rates of 0.3, 0.5, 0.7, 1.0 mV s^{-1} for MoS_2/C

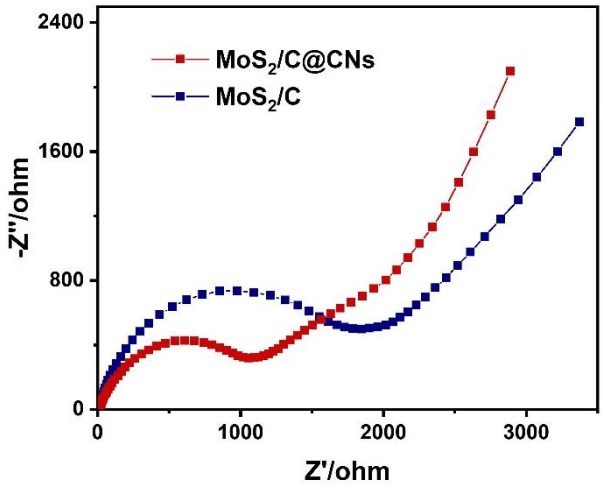

Supplementary Figure S12. EIS spectra of MoS_2/C@CNs and MoS_2/C for PIBs.

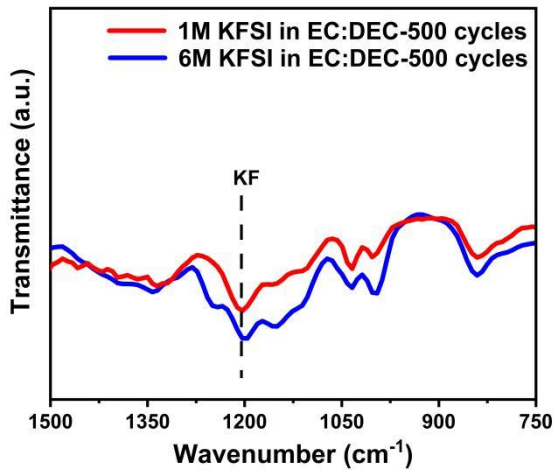

Supplementary Figure S13. FT-IR spectra of discharged MoS_2/C@CNs electrodes in different electrolytes

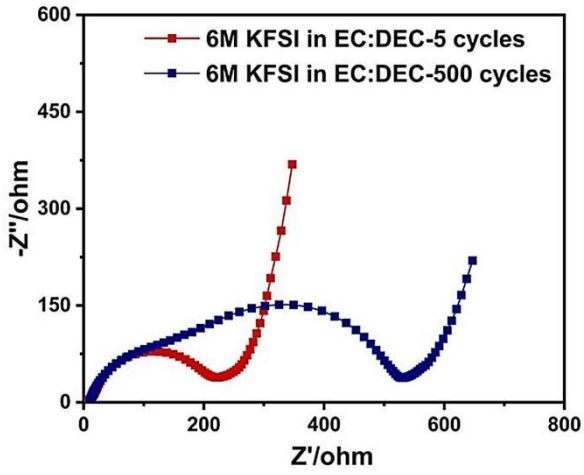

Supplementary Figure S14. EIS spectra of MoS_2/C@CNs electrodes in the concentrated electrolyte after different cycles

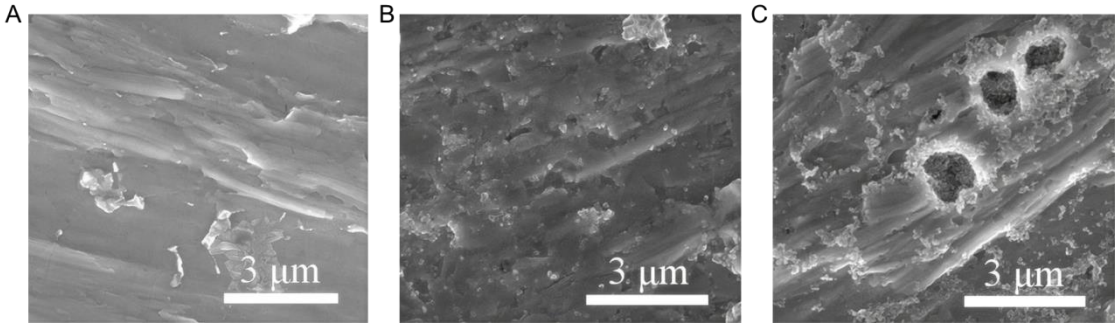

Supplementary Figure S15. SEM images of (A) clean empty copper, (B) copper collector cycled at 200 mA g^{-1} after 500 cycles in 1M KFSI in EC : DEC, (C) and 6M KFSI in EC : DEC

Supplementary Table 1. Comparison of the electrode performance of MoS_2/C@CNs with previously reported PIB anodes.

Materials	**Current density**	Cycles	**Reverse capacity**	Reference

	(mA g^{-1})		(mAh g^{-1})	
MoS_2@HPCS	500	100	254.9	[S1]
MoS_2/N-doped-C	100	200	212	[S2]
MoS_2/C@NDG	1000	150	220.7	[S3]
PCP30@MoS_2	500	100	248.43	[S4]
MoS_2⊂C	2000	150	192.01	[S5]
MoS_2/NGA	100	80	349	[S6]
MoS_2/SNC	500	1200	106	[S7]
MoS_2-WS_2-C	200	100	350	[S8]
E-MoS_2/NOC TC	250	300	220	[S9]
Sn-MoS_2/C	100	50	239	[S10]
MoS_2/C@CNs	**200**	**400**	**315**	**This work**
	2000	**2000**	**164**	

REFERENCES

[S1] Hu J, Xie Y, Zhou X, et al. Engineering hollow porous carbon-sphere-confined MoS_2 with expanded (002) planes for boosting potassium-ion storage [J]. ACS applied materials & interfaces, 2019, 12(1): 1232-1240.https://doi.org/10.1021/acsami.9b14742.

[S2] Jia B, Yu Q, Zhao Y, et al. Bamboo-like hollow tubes with MoS_2/N-doped-C interfaces boost potassium-ion storage [J]. Advanced Functional Materials, 2018, 28(40): 1803409. https://doi.org/10.1002/adfm.201803409.

[S3] Zhang J, Cui P, Gu Y, et al. Encapsulating carbon-coated MoS_2 nanosheets within a nitrogen-doped graphene network for high-performance potassium-ion storage [J]. Advanced Materials Interfaces, 2019, 6(22): 1901066. https://doi.org/10.1002/admi.201901066.

[S4] Jiang Q, Wang L, Chen J, et al. Enhancing potassium-ion battery performance by MoS_2 coated nitrogen-doped hollow carbon matrix [J]. Journal of Alloys and Compounds, 2021, 855: 157505. https://doi.org/10.1016/j.jallcom.2020.157505.

[S5] Hu R, Fang Y, Zhu K, et al. Carbon coated MoS_2 hierarchical microspheres enabling fast and durable potassium ion storage [J]. Applied Surface Science, 2021, 564: 150387. https://doi.org/10.1016/j.apsusc.2021.150387.

[S6] Dong X, Xing Z, Zheng G, et al. MoS_2/N-doped graphene aerogles composite anode for high performance sodium/potassium ion batteries [J]. Electrochimica Acta, 2020, 339: 135932. https://doi.org/10.1016/j.electacta.2020.135932.

[S7] Du Y, Zhang Z, Xu Y, et al. Metal sulfide-based potassium-ion battery anodes: storage mechanisms and synthesis strategies [J]. Acta Phys-Chim Sin, 2022, 38(11): 2205017. https://doi.org/10.3866/PKU.WHXB202205017.

[S8] Choi J H, Park G D, Kang Y C. Potassium-ion storage mechanism of MoS_2-WS_2-C microspheres and their excellent electrochemical properties [J]. Chemical Engineering Journal, 2021, 408: 127278. https://doi.org/10.1016/j.cej.2020.127278.

[S9] Zheng N, Jiang G, Chen X, et al. Rational design of a tubular, interlayer expanded MoS_2-N/O doped carbon composite for excellent potassium-ion storage [J]. Journal of materials chemistry A, 2019, 7(15): 9305-9315. https://doi.org/10.1039/C9TA00423H.

[S10] Yin D, Chen Z, Zhang M. Sn-interspersed MoS_2/C nanosheets with high capacity for Na^+/K^+ storage [J]. Journal of Physics and Chemistry of Solids, 2019, 126: 72-77. https://doi.org/10.1016/j.jpcs.2018.10.029.